Journal of Applied Mechanical Engineering
ISSN: 2168-9873

Fatih KAYA et al., J Appl Mech Eng 2014, 3:1
DOI: 10.4172/2168-9873.1000137

Research Article Open Access

Numerically Modeling of Anode Supported Tubular SOFC

M Fatih KAYA[1*], Nesrin DEMIR[2], Gamze GENÇ[2] and Hüseyin YAPICI[2]

[1]Erciyes University, Department of Mechanical Engineering, 38039 Melikgazi/ Kayseri, Turkey
[2]Erciyes University, Department of Energy Systems Engineering, 38039, Kayseri, Turkey

Abstract

Numerical models of Solid Oxide Fuel Cells (SOFCs) are important tools in understanding and investigate the effect of design and operation parameters of the SOFC performance and SOFC development works. In this study, one of the clean and highly efficient energy production systems, single tubular anode-supported SOFC is modeled numerically. Mathematical model of the single tubular SOFC is given in terms of the incompressible Navier-Stokes, Knudsen diffusion models, Butler–Volmer kinetic equations and Brinkman equations. For two-dimensional axisymmetric geometry, operating conditions, parameters of fuel cell and governing equations are solved by finite element method software ComsolMultiphysics. Pure H_2 89% and H_2O 11% are used at anode and air is used at the cathode side as reactant gasses. Temperature, pressure, porosity, permeability and especially distance of current collectors to the cell reactant gas inlet are studied. Optimal cell parameters for this model are determined and reasons of cell performance effects are explained.

Keywords: Tubular solid oxide fuel cell; Fuel cell; Simulation

Nomenclature

F	Faraday constant	(C/mol)
V	Voltage	(Volt)
I	Current	(Amper)
N	Transferred per mole electron	--
R	Ideal gas constant	(8.3145 J/(mol K))
R_{ohmik}	Ohmic losses	(Volt)
R_{akt}	Activation losses	(Volt)
R_{kon}	Concentration losses	(Volt)
R_{mix}	Mixing ratio	--
P	Pressure	--
E_0	Standart cell potential	(Volt)
I	Exchange current density	(A/m^2)
φ_{rev}	Reversible cell potential	(Volt)
$\varphi_{electrode}$	Electrode potential	(Volt)
φ_{ele}	Electrolyte potential	(Volt)
η	Polarization losses	(Volt)
R	Resistance	(Ohm (Ω))
$D_{i,j}$	Diffusion coefficient	(m^2/sn)
$N_{i,j}$	Molar flow ratio	(cm^2/s)
Δ	Diffusion distance	--
A	Active surface area	(A/cm^2)
ρ	Density	(kg/m^3)
u	Velocity vector	(m/sn)
ω_i	Mass flow	
R_i	Production and consumption ratio	--
j_i	Flow depends on Mass velocity ratio	(kg/m^2s)
ε	Porosity	--
M_i, M_j	Molar mass	(kg/mol)
S_i	Species	--
μ	Dynamic viscosity	(Pa.s)
K	Permeability	(m^2/sn)
rp	Diameter of the porous space	(m^2)
D_K	Knudsen Diffusion	(m^2/sn)
$D_{i,eff}$	Effective diffusion	(m^2/sn)
β	Charge transfer coefficient	--
Σ	Conductivity	(S/m)
T	Temperature	(°C)
$\vec{n}$	Perpendicular vector to the boundary	--

Introduction

Generating energy from clean, renewable and environmental-friendly sources are one of the most important engineering problems. Hydrogen is one of the most abundant and the simplest energy carrier element. Using the energy of hydrogen effectively is a vital factor to prevent destructive effect of global warming. Since 80% efficient values, fuel cells which are converts chemical energy of fuels directly electrical energy, will have a major role next years. Easy to use on mobile

***Corresponding author:** M Fatih Kaya, Erciyes University, Department of Mechanical Engineering, 38039 Melikgazi/Kayseri, Turkey, Tel: +90 352 207 66 66; E-mail: kayamehmetfaith@erciyes.edu.tr

Received October 04, 2013; **Accepted** January 23, 2014; **Published** February 01, 2014

Citation: Fatih KAYA M, Nesrin DEMIR, Gamze GENÇ, Hüseyin YAPICI (2014) Numerically Modeling of Anode Supported Tubular SOFC. J Appl Mech Eng 3: 137. doi:10.4172/2168-9873.1000137

applications and obtain higher power density via power stations make fuel cells applicable and commonly used. Compared with another energy conversion device, high efficiencies of fuel cells can be reached, also for rather small units make fuel cells attractive energy conversion systems [1]. Fuel cells work on lower temperature also may work higher temperature depend on electrolyte material. There are several number of group for fuel cells. Higher efficiency value, SOFCs which are operating higher temperature 600-1000°C have many advantages.

In case of their higher operating temperatures, SOFCs, can convert chemical energy via different kinds of fuels without combustion, such as hydrogen, natural gas, and ethanol [2-5]. They can be produce planar and tubular geometry. Advantages of tubular SOFC versus planar geometry mainly consist of higher power density and no need for sealing materials. The layers of fuel cell specially triple phase boundaries are responsible for converting chemical energy to electrical energy, for this reason thickness, density and characteristic and the numerical modeling of the reaction which occur on these layers are important parameters to increase the performance of fuel cell [6].

In recent years there are lots of works to developing design and performance criteria of SOFCs [7]. These works are generally modeling to predict experimental works. Fuel cells are electrochemical devices, for that there are lots of factor effecting their working performance. Models which are developed for this aspect decreasing performance losses and optimization of some parameters are done. In literature modeling works are generally aimed to decrease costs [8] and investigating the cell working parameters before the experiments [9]. Modelling works done for not only all components of fuel cell but also every single components of SOFCs [10-13].

In this study temperature, pressure, porosity, permeability and distance of current collectors to the cell reactant gas inlet area are studied using COMSOL finite elements method software, Battery and Fuel Cell Module.

Mathematical modeling of tubular SOFC

In Figure 1 axis symmetrical tubular SOFC is demonstrated. In this work, NiO-YSZ is used at the anode side, YSZ is used at the electrolyte and at the cathode side LSM was. Axisymmetric geometric problem is chosen to better and easy solutions for numerical calculations.

In this work:

- Model is in steady state situations and H_0-H_2O mixture is used at the anode side and air is used at the cathode site.

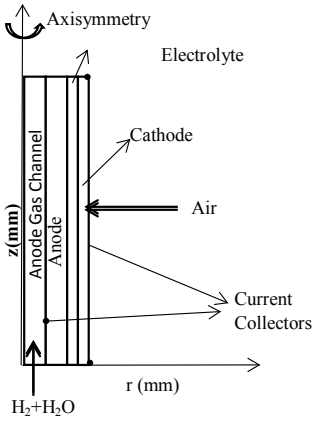

Figure 1: Fuel cell geometry.

- Flow in channels are laminar, reactant gasses are ideal and non-compressible.
- Model is under isothermal condition and cell working temperature is 800°C

Conservation of momentum

Porous flows on the model walls we used Brinkman equation which is derived from the Darcy's Law [14-18].

$$\nabla P = \mu \nabla^2 u + \left(\frac{\mu}{K}\right) u \tag{2.1}$$

$$P = P_{atm} \tag{2.2}$$

$$u \,.\, n = u0 \tag{2.3}$$

Conservation of species

Flow on the porous media generally described with molecular diffusion or Knudsen diffusions [19].

$$D_{i.eff} = \frac{\varepsilon}{\tau}\left(\frac{1}{D_{i,m}} + \frac{1}{D_K}\right)^{-1}\left[\frac{m^2}{s}\right] \tag{2.4}$$

$$D_K = 97 * rp\left(\frac{T}{M_i}\right)^{0.5}\left[\frac{m^2}{s}\right] \tag{2.5}$$

Non-reacting sides in the SOFC steady state diffusion and conduction equations are used.

$$\nabla(-D_i \nabla c_i + c_i u)n = 0 \tag{2.6}$$

At the outside of the anode steady state equations are used.

$$(-D_{kanal,m} \nabla c_i + c_i u)n = 0 \tag{2.7}$$

In the reacting side in fuel cell conservation of species estimated with these equations.

$$(-D_{H_2 a} \nabla cH_2 + cH_2 u) \,.\, n = R_{H_2} \tag{2.8}$$

$$(-D_{H_2 0_a} \nabla cH_2 0 + cH_2 0\, u) \,.\, n = R_{H_2 0} \tag{2.9}$$

$$Ri = \frac{iA}{nF} \tag{2.10}$$

At the cathode-electrolyte interface equations below applied to investigate concentration ratio of oxygen.

$$(-D_{O_{2c}} \nabla cO_2 + cO_2 u) \,.\, n = R_{O_2} \tag{2.11}$$

Boundary conditions for conservation of species at the inlet of anode side take into account the concentration of reacting gasses.

$$cH_2 = cH_{2,0} \tag{2.12}$$

$$cH_2 = cH_2 O_o \tag{2.13}$$

At the cathode side O_2 concentration is used.

$$cO_2 = cO_{2,0} \tag{2.14}$$

Conservation of charge

If current production is only electrode-electrolyte interface and ohmic losses are just in electrolyte, electrode and current collectors, charge conservation at anode side can be described with equation below.

$$-\nabla(\sigma_{a,c}(\nabla \varphi_{a,c})) = 0 \tag{2.15}$$

At the anode-electrolyte interface,

$$-\sigma_{a,c}\nabla\varphi_{a,c}\,.\,n=-i_{a,c} \tag{2.16}$$

The boundary condition at the anode-electrolyte interface,

$$-\sigma_{ele}\nabla\varphi_{ele}\,.\,n=i_{a,c} \tag{2.17}$$

Conductivity equation for anode side

$$-\sigma_{a,c}=\left(\left(\frac{95*10^{6}}{T}\right)*\exp\left(\frac{-1150}{T}\right)\right)\left[\frac{s}{m}\right] \tag{2.18}$$

Conductivity equation for electrolyte side

$$-\sigma_{elek}=\left(\left(\frac{3.34*10^{4}}{T}\right)*\exp\left(\frac{-10300}{T}\right)\right)\left[\frac{s}{m}\right] \tag{2.19}$$

Boundary condition of current collector,

$$\varphi_{anode}=0 \tag{2.20}$$

Other boundaries at the anode side,

$$-\sigma_{a,c}\nabla\varphi_{a,c}\,.\,n=0 \tag{2.21}$$

Charge at the electrolyte equals to zero,

$$-\nabla(\sigma_{ele}\nabla\varphi_{ele})=0 \tag{2.22}$$

Other electrolyte boundaries,

$$-\sigma_{ele}\nabla\varphi_{ele}\,.\,n=0 \tag{2.23}$$

Electronic charge at the cathode equals to zero,

$$-\nabla(\sigma_{c,a}\nabla\varphi_{c,a})=0 \tag{2.24}$$

Cathode-electrolyte side boundary equation,

$$-\sigma_{ele}\nabla\varphi_{ele}\,.\,n=-i_{c,a} \tag{2.25}$$

Cathode current density at the cathode-electrolyte interface,

$$-\sigma_{c,a}\nabla\varphi_{c,a}\,.\,n=i_{c,a} \tag{2.26}$$

At the cathode current collector, boundary condition equals to V_{cell},

$$\varphi_{c,a}=V_{cell} \tag{2.27}$$

Other part of the cathode side boundary conditions,

$$-\sigma_{c,a}\nabla\varphi_{c,a}\,.\,n=0 \tag{2.28}$$

Conductivity of cathode side,

$$\sigma_{c,a}=\left(\left(\frac{42*10^{6}}{T}\right)*\exp\left(-\frac{1200}{T}\right)\right)\left[\frac{s}{m}\right] \tag{2.29}$$

Model validation

In order to observe validation of model the same geometry and cell working conditions are applied than compared with Cheng et al. [19]. As seen in Figure 2, model and Cheng et al. results are agree with each other.

Numerical Results and Discussions

Effect of cell temperature

For this model in Figure 3 shows the effect of cell temperature, increasing temperature from 700 to 800°C the performance of the cell rises. In case of that increasing temperature to 1000°C cell performance decreasing the cause of entropy, decreasing the viscosity of gas reactants and change of effective diffusivity with temperature. In addition increasing temperature reduces the mobility of SOFCs.

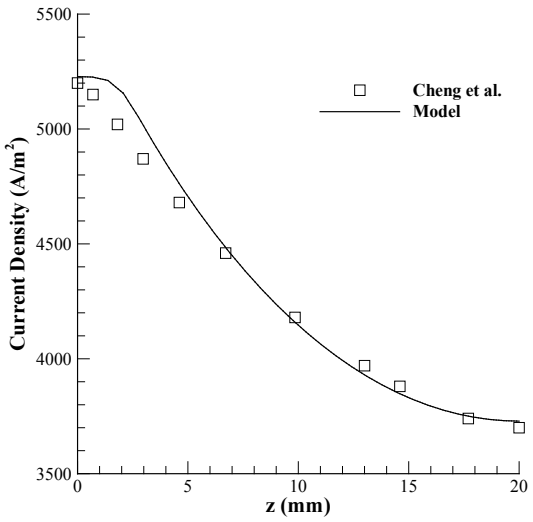

Figure 2: Validation of model with Cheng et al.

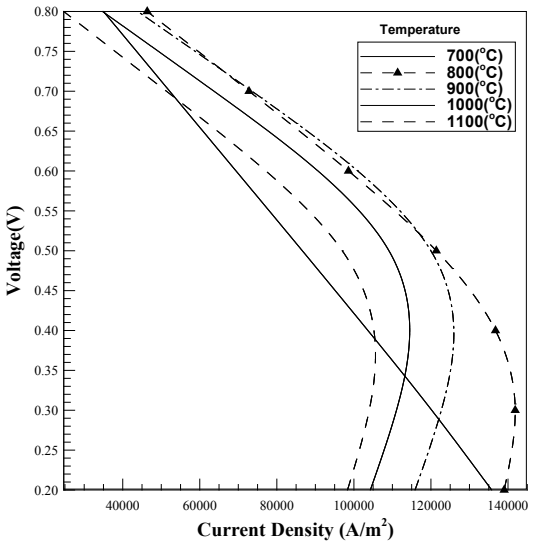

Figure 3: Effect of cell temperature.

Effect of cell reactant pressure

In Figure 4 increasing the cell working pressure, cell performance increases. Higher pressure values increase the Nerst voltage; this is the most important reason of increasing cell performance. At the same time, diffusion of species and concentration are increasing.

Effect of cathode electrode porosity

Another important factor of cell performance is porosity value of electrodes. In this work, anode porosity is constant and this value is 0.3, cathode porosity is changed between 0.2-0.5. Electrode porosity has lower effect for performance than other cell working factors. As seen in Figure 5 for 0.4 and 0.5 porosity value, result of the big gaps between particles which conduct electricity, cell performance reduces whereas between 0.2-0.3 value cell performance not increases significantly.

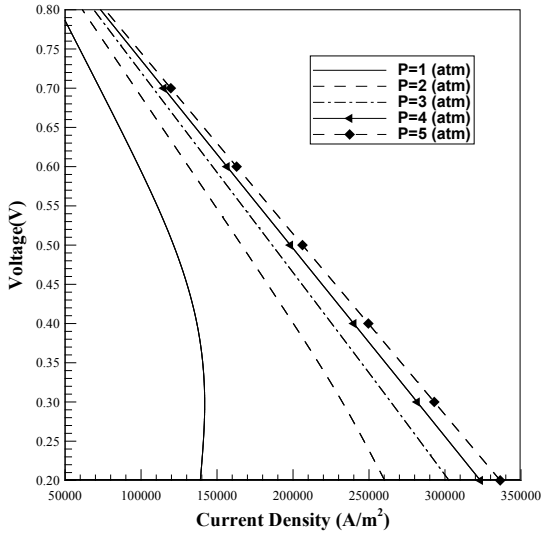

Figure 4: Effect of pressure.

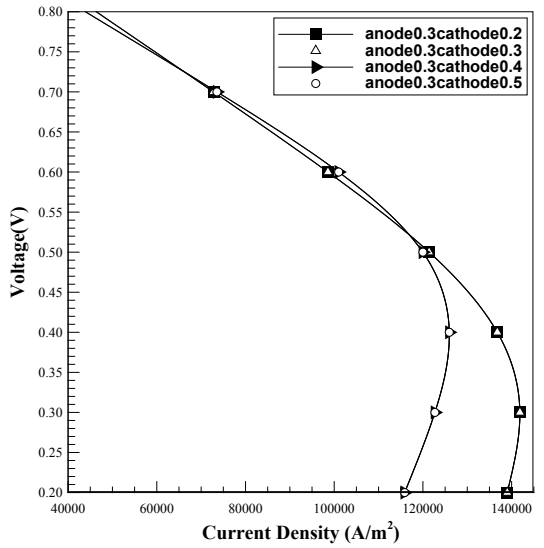

Figure 5: Effect of electrode porosity.

Effect of permeability

Effect of permeability is more important than porosity values. Permeability is the function of the thickness of electrode layer and the pressure drops. In Figure 6 changing permeability between 10-15-10-12 cell performance increases the result of the decreasing flow resistances in porous media (Tables 1-3). Decreasing flow resistance causes the more reactant transfer to the reaction site.

Effect of current collector distance to the cell reactant inlet area

Figure 7 depicts the effect of current collector distance to inlet area, increasing step by 0.5 mm between 1.5-3.5 mm. As a result, it can be seen from the figure, current density changes with opposite direction with length of current collectors. It is the reason of the ohmic losses, causing the bigger contact resistance of current collector surface.

Conclusions

SOFCs generally work between 600-1000°C cell temperatures. In this work we observed maximum performance value is between 800-900°C. Higher temperature values caused decreasing of cell performance as a result of changing the diffusion, viscosity, concentration, density and conductivity values. However, higher the cell pressure, cell performance is increased due to the bigger value of Nerst voltages. As well as higher pressure value increase the concentration value of ideal gasses. For this reason exchange current density is increased. In addition porosity values are another factor of performance of fuel cell, but porosity value is not effective like other parameters. 0.2-0.3 values have better results for cell working conditions. Permeability is more important parameter, increasing this parameter in experimental procedures, performance will increase slightly. Distance of current collector surface to r axis is another vital factor for causing ohmic losses. Lower surface areas of current collection implement higher power density for fuel cells.

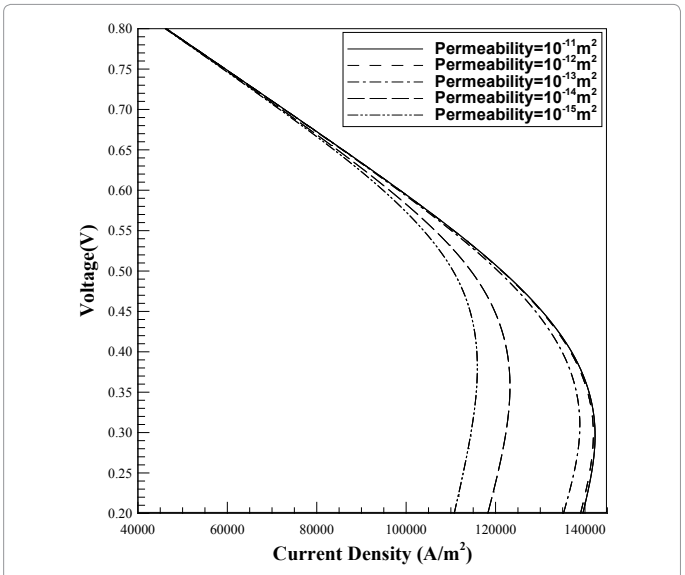

Figure 6: Effect of permeability.

Species	ε	τ	K (m²)	rp (m)
Anode	0.3	10	1E-12	5E-7
Electrolyte	0.001	-	-	-
Cathode	0.3	10	1E-12	5E-7

Table 1: Porous Media Parameters.

P (atm)	V_{cell} (V)	T (°C)
1	0.8	800

Table 2: Cell Boundary Parameters.

Species	$D_{(i,j)}\left(\frac{m^2}{s}\right)$	$i_{(i,j,0)}\left(\frac{A}{m^2}\right)$	β
Anode	H_2=3.14E-5	5300	0.5
	H_2O=1.39E-5		
Electrolyte	-	-	-
Cathode	O_2=7.588E-6	2000	0.5
	N_2=7.588E-6		
Flow Channel	8.51E-04	-	-

Table 3: Transfer Parameters.

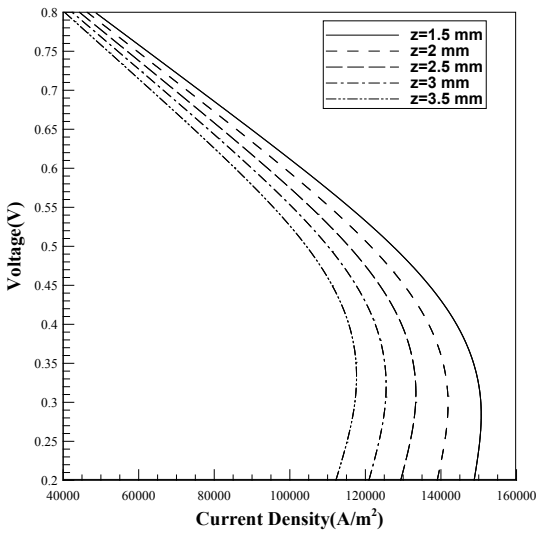

Figure 7: Effect of current collector distance to the cell reactant inlet area.

References

1. Stöver D, Hathiramani D, Vaben R, Damani RJ (2006) Plasma Sprayed Components For SOFC Applications, The 2nd International Meeting on Thermal Spraying 201: 2002-2005.
2. Ivers-Tiffe E, Weber A, Herbstritt DJ (2001) Materials and technologies for SOFC-components, Eur Ceram Soc 21: 1805-2001.
3. Nascimento AC, Basaglia RMF, Cunha FTA, Fonseca CG, Brant MC, et al. (2009) Correlation between yttria stabilized zirconia particle size and morphological properties of NiO–YSZ films prepared by spray coating process, Ceramics International, 35: 3421-3425.
4. Minh NQ, Takahashi T (1995) Science and Technology of Ceramic Fuel Cells, Elsevier, New York, 132-147.
5. Minh NQ (1993) Ceramic fuel cells, J. Am. Cerm. Soc. 76: 563-588.
6. Zielman J, DeMinco C, Mukerjee S,Tachtler J, Kammerer J, Lamp P (2002) in: Marcus Nurdin (Ed.), The Fuel Cell World, Lucerne, Switzerland, 306.2002.
7. Kakaç S, Pramuanjaroenkij A, Zhou XY (2007) A review of numerical modeling of solid oxide fuel cells, International Journal of Hydrogen Energy, 32: 761-786.
8. Lucchese P, VaroquauxA (2001) High temperature SOFC cells: state of the art and prospects, CLEFS CEA 2001, 44: 57-59.
9. Akhtar N (2011) A parametric analysis of a micro-tubular, single-chamber solid oxide fuel cell (MT-SC-SOFC), International Journal of Hydrogen Energy, 36: 765-772.
10. Lehnert W, Meusinger J, Thom F (2000) Modelling of gas transport phenomena in SOFC anodes, Journal of Power Sources, 87: 57-63.
11. Dusastre V, Kilner JA (1999) Optimisation of composite cathodes for intermediate temperature SOFC applications, Solid State Ionics, 126: 163-174.
12. Yakabe H, Ogiwara TM, Hishinuma M, Yasudal (2001) 3-D model calculation for planar SOFC, Journal of Power Sources, 102: 144-154.
13. Huang J, Yuan J, Mao Z (2010) Analysis and Modeling of Novel Low-Temperature SOFC With a Co-Ionic Conducting Ceria-Based Composite Electrolyte, J Fuel Cell Sci Technol., 7: 011012-1.
14. Bove R, Ubertini S (2006) Modelling solid oxide fuel cells methods procedures and techniques, Journal of Power Sources, 159: 543-559.
15. HabermanBA, Young JB (2004) Three-dimensional simulation of chemically reacting gas flows in the porous support structure of an integrated-planar solid oxide fuel cell, International Journal of Heat and Mass Transfer, 47: 3617–3629.
16. Ji Y, Yuan K, Chung JN,Chen YC (2006) Effects of transport scale on heat/mass transfer and performance optimization for solid oxide fuel cells, Journal of Power Sources, 161: 380-391.
17. Clifford KH, Webb SW (2006) Gas transport in porous media, London, 444.
18. EG&G Technical Services Inc, Fuel Cell Handbook. 7th Edition ed. 2004, Morgantown, West Virginia: National Energy Technology Lab, US Department of Energy.
19. CuiD, LiuL, DongY, Cheng M (2007) Comparison of different current collecting modes of anode supported micro-tubular SOFC through mathematical modeling, Journal of Power Sources, 174: 246-254.